Available online at www.sciencedirect.com
SCIENCE DIRECT®
Quaternary International 118–119 (2004) 127–143

Post-glacial evolution of the Indo-Pacific Warm Pool and El Niño-Southern oscillation

Michael K. Gagan[a,*], Erica J. Hendy[a], Simon G. Haberle[b], Wahyoe S. Hantoro[c]

[a] Research School of Earth Sciences, The Australian National University, Canberra ACT 0200, Australia
[b] Department of Geography and Environmental Science, Monash University, Clayton Vic. 3168, Australia
[c] Research and Development Center for Geotechnology, Indonesian Institute of Sciences, Bandung 40135, Indonesia

Abstract

Recent research has revealed new insights into the temperature, size, and variability of the Indo-Pacific Warm Pool (IPWP) and the nature of the El Niño-Southern Oscillation (ENSO) since the Last Glacial Maximum (LGM). Sea surface temperature (SST) reconstructions from foraminiferal Mg/Ca, alkenone, and revised coral Sr/Ca palaeothermometry agree that SSTs in the IPWP during the LGM were ~3°C cooler than at present. In the central portion of the IPWP, the rapid post-glacial rise in SST led the deglaciation by ~3000 years to produce near-modern SSTs by the early Holocene. In contrast, further west and north, post-glacial shifts in SSTs in the South China and Sulu Seas are synchronous with abrupt climate changes in the North Atlantic. New evidence for the nature of the Little Ice Age in the tropics has been obtained from a 420-year record of coral Sr/Ca and $\delta^{18}O$ from the Great Barrier Reef, Australia. This indicates that SSTs and salinity were higher in the 18th century than in the 20th century. The results suggest that the tropical Pacific played a role as a source region of water vapour during the global expansion of Little Ice Age glaciers. The onset of modern ENSO periodicities is identified by palaeo-ENSO records throughout the tropical Pacific region ~5000 years ago, with an abrupt increase in ENSO magnitude ~3000 years ago. Individual ENSO events recorded by corals reveal that the precipitation response to El Niño temperature anomalies was subdued in the mid-Holocene. The apparent non-linear onset of ENSO in the late Holocene appears to reflect abruptly enhanced interaction between the Southern Oscillation and the Pacific Intertropical Convergence Zone. Comparisons of precipitation variability recorded by Great Barrier Reef corals with ENSO indices for the last 350 years confirms that non-stationarity of ENSO teleconnections is a natural characteristic of modern climate.
© 2003 Elsevier Ltd and INQUA. All rights reserved.

1. Introduction

Approximately 11% of the surface of Earth's oceans is covered by water with average annual temperatures exceeding 28°C (Webster, 1994). This relatively warm, fresh, 'skin' of buoyant warm pool water occupies only 0.05% of the total ocean water mass, yet it plays a leading role in driving atmospheric circulation. By far the largest expanse of warm water is encompassed by the Indo-Pacific Warm Pool (IPWP; Fig. 1). Here, the stable layers of the tropical warm pool are, at least in part, a direct result of the precipitation excess in the IPWP region (Webster, 1994). The IPWP is one of the wettest tropical ocean regions on Earth; precipitation exceeds evaporation by ~2 m within the 28°C isopleth (Oberhuber, 1988). The net precipitation effectively stabilises the upper ocean producing a shallow mixed layer in a region of maximum solar heating. In the absence of other factors, the SST of the IPWP should increase unabated. Although still incompletely understood, negative feedbacks including modulation of the radiative heating by clouds, wind-induced evaporation, and upper ocean mixing, appear to modulate the upper limit of sea surface temperature (SST; Ramanathan and Collins, 1991).

What we do know is that the temperature, size, and positioning of the IPWP can have a profound effect on global climate (Cane and Clement, 1999). Fig. 2 (after Webster, 1994) illustrates how the Warm Pool, despite its small size, is a primary component of the global coupled ocean–atmosphere system. Although the fundamental processes linking atmospheric convection and SST are still not known, the genesis of vigorous atmospheric convection begins when SSTs exceed 28°C (Lau and Chan, 1982). Thus collected solar energy is released over the warm pool through vigorous atmospheric convection. This air moves poleward where

*Corresponding author.
E-mail address: michael.gagan@anu.edu.au (M.K. Gagan).

1040-6182/$ - see front matter © 2003 Elsevier Ltd and INQUA. All rights reserved.
doi:10.1016/S1040-6182(03)00134-4

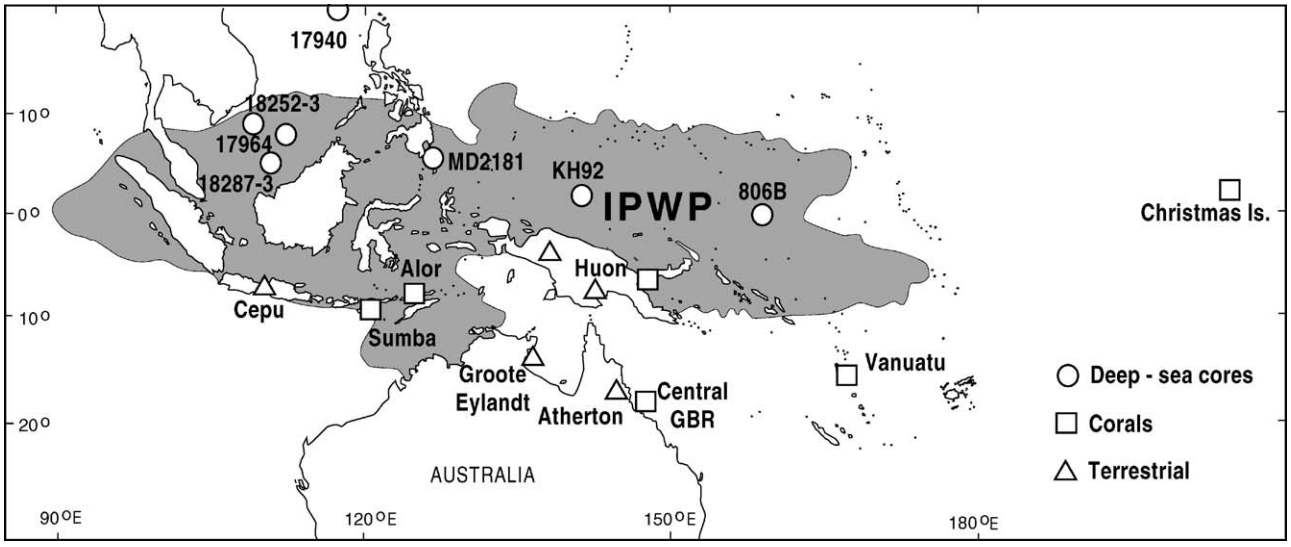

Fig. 1. Locations of deep-sea sediment cores (circles), corals (squares), and terrestrial palaeoclimate records (triangles) from the tropical Indo-Pacific Warm Pool (IPWP) region, and described in Figs. 3,4 and 6–8. Dark stippling marks the average extent of the IPWP (mean annual SST > 28°C), as defined by Yan et al. (1992).

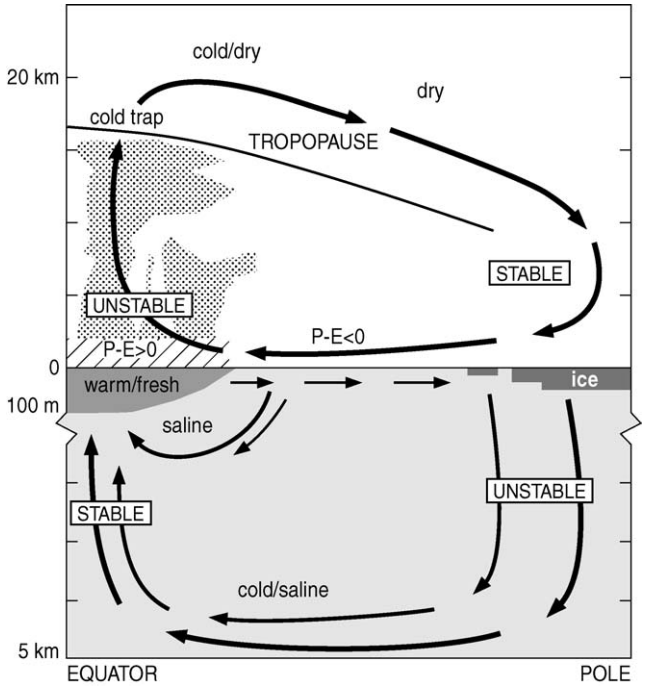

Fig. 2. Cross-section summarising ocean–atmosphere interactions along an equator-to-pole transect and the thermohaline circulation processes involved in maintaining the Indo-Pacific Warm Pool (after Webster, 1994). The Warm Pool water (>28°C) associated with deep atmospheric convection and precipitation in the tropics constitutes only a small fraction of the total ocean water mass (<0.05%). Surface cooling and the formation of sea ice in the polar regions results in the formation of cold saline deep water. Equatorward flow of deep water and subduction of saline water from the subtropics enhances the stability of the warm pool and helps to maintain high SSTs in the tropics.

it subsides and warms adiabatically to create a stable inversion layer over the poles. Rapid surface cooling in the polar regions and the formation of sea ice (through salt rejection) allows the remaining relatively dense surface water to mix downward (deepwater formation). The resulting pole-to-equator thermohaline circulation transports water away from the poles, which then ascends toward the equator. Thus the relative buoyancy and stability of the Warm Pool is maintained by two hydrologic processes, heat and freshwater fluxes at the upper ocean surface and cold, saline deep ocean water rising from below. The resulting stability of the thermocline (and halocline) below the warm pool helps maintain the warm SSTs of the tropical surface ocean.

A crucial issue in global climate change research is to reconstruct tropical SSTs and the locus of atmospheric convection in the tropics. Because centres of tropical convection tend to lie over the warmest water, changes in the temperature, size, and location of the IPWP should alter the impacts of climate change on distant locations (Clement et al., 2001). Until recently, it was believed that SSTs in the tropics varied little over glacial-interglacial time-scales (CLIMAP, 1981). However, during the last decade new isotopic and elemental palaeothermometers have revealed that this is not the case. It is now thought that the role of the tropics in global climate variability spans interannual (El Niño-Southern Oscillation; ENSO) to millennial time-scales (Cane and Clement, 1999).

In this paper, we begin by reviewing the most recent estimates of SST variability in the IPWP region since the Last Glacial Maximum (LGM) and during the Little Ice Age (LIA). Having established the nature of the evolving mean climate of the IPWP, we then examine the information provided by terrestrial and marine proxy records of ENSO. Comparison of proxy records with model simulations of the Holocene ENSO provides insight into areas of agreement. Where data and models

agree, the processes involved in forcing changes in the ENSO can be determined. The last section of the paper reviews new coral evidence for the evolving strength of ENSO teleconnections in northeast Australia since the mid-17th century.

2. Post-glacial temperature history of the Indo-Pacific Warm Pool

2.1. Palaeothermometry

Three promising new palaeothermometers have led to important findings about the temperature history of the IPWP since the LGM, and beyond; Mg/Ca in surface-dwelling foraminifera, alkenone unsaturation ratios, and Sr/Ca in corals. Studies of foraminiferal Mg/Ca and alkenones from deep-sea sediment cores have the advantage of providing long, continuous histories of changes in mean SST (Ohkouchi et al., 1994; Pelejero et al., 1999; Lea et al., 2000; Kienast et al., 2001; Stott et al., 2002). In contrast, corals provide high resolution 'windows' into past climate spanning decades to centuries, at monthly or better temporal resolution (Gagan et al., 2000). Recently, these palaeothermometers have been used to remove the temperature component of the oxygen isotope signal in biogenic carbonates and thereby reveal changes in seawater ^{18}O concentrations as a proxy for surface-ocean salinity (e.g., Gagan et al., 1998; Lea et al., 2000; Hendy et al., 2002; Stott et al., 2002).

The temperature dependence of the substitution of Mg in foraminiferal shell calcite has been calibrated through culturing to reveal a response of ~9% per °C, which is easily measured by inductively coupled plasma mass spectrometry (ICP-MS; Lea et al., 1999). Although Mg/Ca palaeothermometry has only been applied widely during the last 5 years, several novel findings are already at hand. We review the primary findings from a planktonic foraminiferal Mg/Ca record from the Ontong Java Plateau in the western sector of the IPWP (Fig. 1; Lea et al., 2000).

The production of unsaturated alkenones (ketones) in the cell membranes of some marine phytoplankton responds to changes in water temperature and provides a good cross-check for palaeotemperatures derived from Mg/Ca in foraminifera. The temperature dependent unsaturation index (U^{k}_{37}) derived from phytoplankton in deep-sea sediments has been used to estimate temperatures in the photic zone (upper 10 m of water column). Although the sensitivity of C_{37} alkenones to changes in tropical SSTs decreases in the warmest regions (i.e., warm pool), sedimentary C_{37} alkenone ratios provide good estimates where production rates are high (Pelejero and Grimalt, 1999). Alkenone records are now available for the southern South China Sea (Pelejero et al., 1999) and Sulu Sea (Kienast et al., 2001) located in the northern sector of the IPWP.

The use of Sr/Ca in coral skeletons as a palaeothermometer came to fruition in the early 1990s when precise thermal ionisation mass spectrometric (TIMS) determinations were used to establish the relationship between small changes in coral Sr/Ca and temperature (~0.6% per °C; Beck et al., 1992). Since then, a number of laboratories have used the coral Sr/Ca thermometer to reconstruct the temperature history of the tropics. We review recent temperature estimates for the IPWP region, including data sets from Vanuatu (Beck et al., 1992, 1997; Corrège et al., 2000), Papua New Guinea (McCulloch et al., 1996), the Great Barrier Reef (Gagan et al., 1998), and eastern Indonesia (M. Gagan, unpublished data). We also review the use of the Sr/Ca thermometer to reconstruct SST variability in the southwest Pacific over the last four centuries (Linsley et al., 2000; Corrège et al., 2001; Hendy et al., 2002).

2.2. Dating methods

Recent advances in radiocarbon dating and uranium-series geochronology have led to significant improvements in chronological control for palaeoceanographic studies. Radiocarbon concentrations, determined precisely on milligram quantities of carbonate by accelerator mass spectrometry (AMS), are now widely used to directly date foraminifera in deep-sea cores. In the studies reviewed below, a mean tropical oceanic reservoir correction of 400 years has been subtracted from the conventional radiocarbon age. Oceanic reservoir corrected ages were then converted to calendar years (calendar yr BP.) according to Stuiver and Reimer (1993) for comparison with uranium-series age determinations.

Precise calendar ages for fossil corals can be obtained by measuring $^{230}Th/^{234}U$ ratios by thermal ionisation mass spectrometry (Edwards et al., 1987). Errors associated with ^{230}Th age determinations are generally less than 1% for well-preserved coral samples spanning the last glacial cycle. Ages for the coral records reviewed below have been determined using uranium-series geochronology and are comparable with oceanic reservoir corrected foraminiferal radiocarbon ages, after conversion to calendar years BP.

2.3. Post-glacial temperature history

2.3.1. Foraminiferal Mg/Ca

Fig. 3 summarises palaeotemperature estimates for the warm pool region since the LGM, based on foraminiferal Mg/Ca, alkenone unsaturation ratios, and coral Sr/Ca. Two foraminiferal Mg/Ca records are now available for the IPWP region; one from ODP Hole 806B on the Ontong Java Plateau (Lea et al., 2000),

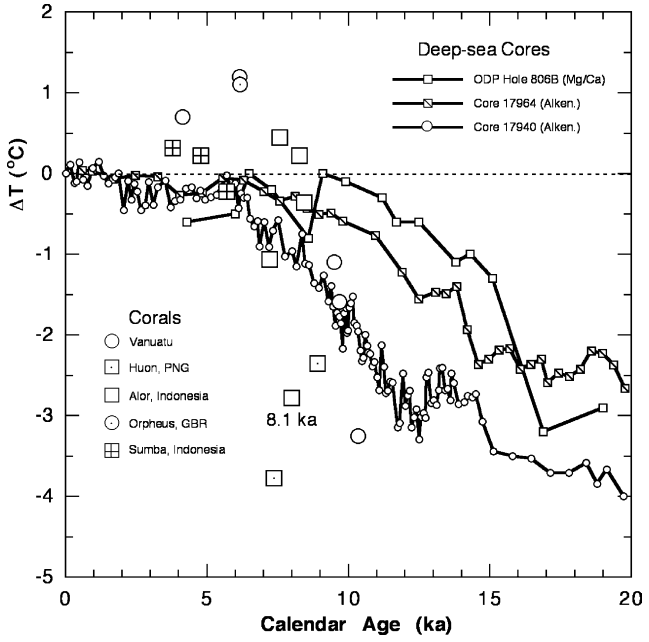

Fig. 3. Comparison of reconstructed SSTs, relative to late 20th century values, in the IPWP region during the last 20,000 years using foraminiferal Mg/Ca, alkenone, and coral Sr/Ca thermometry. Calcite Mg/Ca was measured for the surface-dwelling planktonic foraminifer *Globigerinoides ruber* in ODP Hole 806B on the Ontong Java Plateau (0°19.1′N, 159°21.7′E) near the centre of the IPWP (after Lea et al., 2000). Conversion of core depth to age is based on estimated age of the core-top and correlation of the *G. ruber* δ^{18}O record to the planktonic SPECMAP δ^{18}O curve (Imbrie et al., 1984). Reconstructed SSTs for the southern South China Sea are based on application of the U^{K}_{37} index to C_{37} long chain alkenones in two deep-sea sediment cores (Core 17694: 6°09′N, 112°13′E; Core 17940: 20°07′N, 117°23′E) collected during the *Sonne* 95 cruise (after Pelejero et al., 1999). Sediment core age models are based on accelerator mass spectrometer (AMS) ^{14}C dates calibrated to calendar years before the present, and foraminiferal δ^{18}O stratigraphy. Coral Sr/Ca estimates of SST are based on fossil specimens of *Porites* from Espiritu Santo, Vanuatu (15°40′S, 167°E; Beck et al., 1997; Corrège et al., 2000); Huon Peninsula, Papua New Guinea (6°S, 147°E; McCulloch et al., 1996); Orpheus Island, Great Barrier Reef (18°34′S, 146°29′E; Gagan et al., 1998); Alor, southern Indonesia (8°14′S, 124°24′E), and Sumba, southern Indonesia (09°28′S, 120°06′E). ^{230}Th/^{234}U calendar ages for corals were determined by thermal ionisation mass spectrometry (TIMS). The relationship for converting coral Sr/Ca to SST is: $T(^{\circ}C) = 168.2 - [15,674^{*}(Sr/Ca)_{atomic}]$, which has been derived for modern *Porites* specimens from open-water continental and island arc fringing reefs throughout the Indo-Pacific region (Gagan et al., 1998).

which lies near the equator in the eastern sector of the warm pool, and another core (MD2181) collected by the IMAGES program south of the Philippines in the central sector of the IPWP (Stott et al., 2002). An estimated cooling of 2.8 ± 0.7°C during the LGM was derived from Mg/Ca in *Globigerinoides ruber* from the Ontong Java Plateau. This result has recently been verified by the foraminiferal Mg/Ca temperature estimates for the south Philippines, where summer temperatures during the LGM (based on Mg/Ca in *G. ruber*) were ~2°C cooler than late Holocene temperatures. Winter temperatures based on Mg/Ca in *G. sacculifer* were ~3°C cooler.

Taken together, the results suggest that the near-equatorial portion of the warm pool cooled by 2–4°C during the LGM. Interestingly, both cores show a rapid rise to early Holocene SSTs which were as warm as modern values (Fig. 3). Comparisons of Mg/Ca and δ^{18}O measured in the same foraminifers in both cores clearly indicate that the rise in SST in the core of the IPWP led deglaciation by ~3000 years (Lea et al., 2000; Stott et al., 2002).

2.3.2. Alkenones

In general, the results of alkenone unsaturation palaeotemperature estimates for the IPWP region are consistent with the 3°C cooling during the LGM indicated by foraminiferal Mg/Ca. Alkenone unsaturation ratios for a sediment core located north of Papua New Guinea, in the central Warm Pool, indicate a maximum cooling of 1.5°C during the LGM (Ohkouchi et al., 1994). However, very warm oligotrophic tropical sites, such as the core of the warm pool, are poor candidates for the alkenone palaeotemperature approach because of the subdued sensitivity of alkenones to temperature at high SSTs (Pelejero and Grimalt, 1999). In contrast, alkenone palaeotemperature estimates from the South China Sea, where the production of C_{37} alkenones is high, are in much better agreement with the foraminiferal Mg/Ca. Several cores in the southern sector of the South China Sea (5–10°N) yield LGM cooling of ~3°C (Pelejero et al., 1999; Kienast et al., 2001). Further north (21°N), the LGM cooling increases to 4–5°C (Pelejero et al., 1999). Like the foraminiferal Mg/Ca, the alkenone records show SSTs within 1°C of modern values by the early Holocene.

In contrast to the central IPWP, the post-glacial SST rise in the South China Sea does not appear to lead deglaciation. Changes in the high-resolution alkenone records are synchronous with the typical North Atlantic Termination I features, with well-defined Bølling-Allerød and Younger Dryas events (Pelejero et al., 1999; Kienast et al., 2001). The Younger Dryas also has been identified in foraminiferal δ^{18}O records from the nearby Sulu Sea (Linsley and Thunell, 1990; Kudrass et al., 1991; Linsley, 1996). Thus, the available evidence suggests that the South China Sea and Sulu Sea respond to Northern Hemisphere forcing, perhaps under the influence of the changing Asian monsoon (Wang et al., 1999; Kienast et al., 2001). On the other hand, apparently the 'open-ocean' portion of the IPWP was not under the direct influence of the Northern Hemisphere deglaciation.

2.3.3. Coral Sr/Ca

Estimating mean SST in the tropical western Pacific during the post-glacial transition using coral Sr/Ca

palaeothermometry has been controversial because early estimates indicated cooling as great as 6°C, even as late as the early Holocene (Beck et al., 1992, 1997). It is likely that systematic differences between Sr/Ca-temperature calibrations for the coral genus *Porites* have exaggerated the degree of LGM cooling indicated by coral Sr/Ca for the western Pacific. Recent work has shown that Sr uptake in coral skeletons is reduced by light-enhanced calcification, resulting in artificially warm SST estimates (Cohen et al., 2001). Thus one potential problem with SST estimates from fossil corals is that modern coral Sr/Ca-SST relationships applied to fossil corals have been derived from modern reef settings with light regimes that are not analogous to those in which the fossil corals grew. So far, the coral Sr/Ca–temperature relationships applied to fossil corals have been derived from modern corals growing in oligotrophic, clear water, high light intensity barrier reef and mid-ocean island reef settings (Beck et al., 1992; de Villiers et al., 1994). In contrast, the fossil coral specimens examined in the western Pacific are invariably from relatively turbid continental and island arc fringing reef environments. In these ancient fringing reef settings, light-enhancement of calcification in corals is likely to be less (greater Sr uptake) than in the modern calibration settings. As a result, SST estimates from fossil corals could be systematically biased towards temperatures that are too cold.

Fig. 3 shows the revised coral Sr/Ca estimates of post-glacial SSTs using a single Sr/Ca-SST calibration derived specifically for application to continental and island arc fringing reefs in the southern IPWP region (Gagan et al., 1998). A clearer picture emerges for the Southern Hemisphere portion of the IPWP when the single calibration equation is applied to fossil coral Sr/Ca data available for Vanuatu (Beck et al., 1997; Corrège et al., 2000), Papua New Guinea (McCulloch et al., 1996), the inshore Great Barrier Reef (Gagan et al., 1998), and two sites in southeastern Indonesia, Sumba (Pirazzoli et al., 1991) and Alor (Hantoro et al., 1994). The Vanuatu coral SST estimates for the early Holocene now indicate cooling of 1–3°C, rather than 4–6°C, as estimated previously using a Sr/Ca-SST calibration based on corals from the barrier reef of New Caledonia (Beck et al., 1997). New coral Sr/Ca records from Alor, southeast Indonesia, show that SSTs reached modern values by ~8.5 ka, in good agreement with the Mg/Ca and alkenones. This generally warm period is interrupted by a brief cold-spike centred on 8.1 ka (M. Gagan, unpublished data). Mid-Holocene SSTs in Indonesia (Sumba) fall within 0.5°C of modern values, whereas corals from the inshore Great Barrier Reef, Australia, indicate SSTs ~1°C warmer than the present.

Although the new coral SST estimates are in much better agreement with the foraminiferal Mg/Ca and alkenone SST estimates, some of the coral records are still significantly cooler or warmer than the deep-sea sediment core estimates. Coral records showing cool SSTs could be recording real changes, particularly coastal upwelling, on time-scales of decades. Cool artifacts may also be produced by possible enrichment of Sr in seawater during the LGM (Stoll and Schrag, 1998), early marine aragonite cements (Müller et al., 2001), and off-axis sampling of coral skeletons (de Villiers et al., 1994). Warm artifacts, on the other hand, may result from vadose-zone calcite diagenesis in corals sampled from uplifted coral terraces (McGregor and Gagan, 2003).

The general agreement between foraminiferal Mg/Ca, alkenone, and coral Sr/Ca records is beginning to reveal a coherent picture of past SST variability in the IPWP. The results indicate strongly that cooling of the IPWP during the LGM was ~3°C, rather than ~4–6°C, as indicated by earlier coral records. It appears that the post-glacial rise in SST to modern temperatures in the early mid Holocene led deglaciation, at least in the 'open ocean' portion of the IPWP (Lea et al., 2000; Stott et al., 2002). Further west and north, SST changes in the South China and Sulu Seas were synchronous with abrupt changes in the Northern Hemisphere (Linsley and Thunell, 1990; Kudrass et al., 1991; Linsley, 1996; Pelejero et al., 1999; Wang et al., 1999; Kienast et al., 2001).

3. The last five centuries: the demise of the Little Ice Age and 20th century warming

In global and hemispheric-scale palaeotemperature reconstructions the 20th century is consistently identified as the warmest century in the last millennium (Jones et al., 1998; Mann et al., 1998, 1999; Crowley, 2000). The anomalous warmth of the 20th century contrasts with its occurrence at the end of a millennium-scale cooling trend (Bradley, 2000; Jones et al., 2001), which culminates between the 15th and late 19th centuries in the Little Ice Age (LIA; Grove, 1988; Crowley and North, 1991; Bradley and Jones, 1993; Lamb, 1995). Most Northern Hemisphere palaeoclimate reconstructions record the LIA as multiple, century-scale periods of unusually cold, dry conditions. Glacial advances in both hemispheres (Grove, 1988) and enhanced polar atmospheric circulation (Kreutz et al., 1997) suggest that the LIA was a global-scale event, though cooler conditions were possibly restricted to higher latitudes (Rind, 1998, 2000). Few of the sparse reconstructions of the LIA available from the tropics identify cold periods synchronous with those in the Northern Hemisphere composite reconstructions (Hendy et al., 2002). Attempts to describe temperature patterns for the Southern Hemisphere as a whole, however, are also

hindered by conflicting signals in the limited number of available proxy-temperature records (Bradley and Jones, 1993; Jones et al., 1998, 2001).

Recent replicated coral proxy records of SST (from Sr/Ca; Fig. 4A) and sea surface salinity (SSS from $\delta^{18}O$; Fig. 4B) anomalies in the tropical southwest Pacific suggest that a dramatic shift occurred in the tropical ocean–atmosphere system at the end of the LIA (Hendy et al., 2002). In addition, the Sr/Ca SST reconstruction demonstrates that the 20th century was not unusually warm in relation to the last 420 years. Although an extended period from AD 1565 to 1700 was ~0.2–0.3°C cooler than the long-term average, a century-scale warming of 0.4°C centred on AD 1700 was followed by above average SSTs that were consistently as warm as the early 1980s. These warm SST anomalies persisted through most of the 18th and 19th centuries before cooling to a minimum in the early 20th century.

The difference between tropical Pacific reconstructions and Northern Hemisphere temperature reconstructions (e.g., Jones et al., 1998; Mann et al., 1999), which are dominated by terrestrial temperate zone proxy sources, led Hendy et al. (2002) to propose that temperature gradients between tropical low latitudes and mid-to-high latitudes were greater during the LIA than for the period since the late 19th century. Positive SST anomalies in the 18th and 19th centuries are seen in the U/Ca-SST reconstruction from the same GBR corals

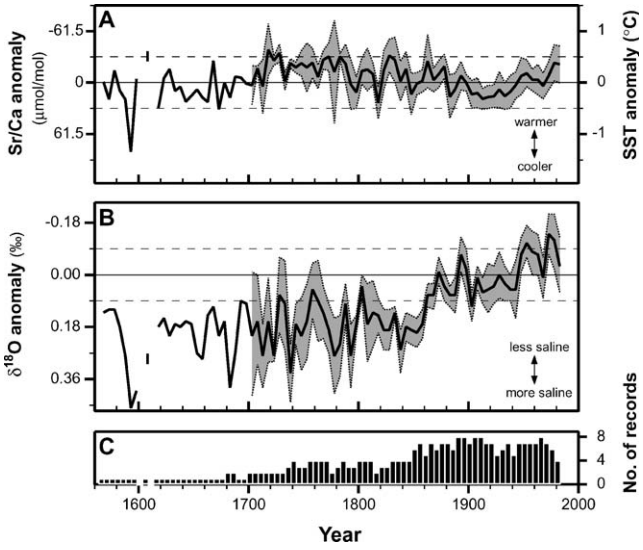

Fig. 4. Composite records of (A) coral Sr/Ca and (B) coral $\delta^{18}O$ for AD 1565–1985 based on eight cores from massive *Porites* colonies from the central GBR, Australia (after Hendy et al., 2002). Solid lines are reconstructions, at pent-annual resolution, normalised to the period 1860–1985 with 95% confidence intervals shaded. The Sr/Ca-SST reconstruction is plotted as ratios (left axis) and SST anomalies (right axis) using the calibration slope of −61.5 µmol/mol per °C (Alibert and McCulloch, 1997; Gagan et al., 1998). Horizontal dashed lines define the ±0.5°C relative to 1860–1985 period. The number of records averaged at each pent-annual interval for the $\delta^{18}O$ reconstruction is given in (C).

(Hendy et al., 2002) and in other coral records across the Pacific, including a Sr/Ca-SST record from Rarotonga (Linsley et al., 2000) and a $\delta^{18}O$-SST reconstruction from Galapagos (Dunbar et al., 1994). On the other hand, a 60-year coral Sr/Ca and U/Ca record from New Caledonia provides conflicting evidence for a 1.4°C cooler climate centred around AD 1730 (Corrège et al., 2001). More coral Sr/Ca and U/Ca-SST records, preferably replicated within sites, from across the tropics are needed to clarify zonal and meridional temperature gradients on decadal to century time scales.

In addition to warm SSTs, Hendy et al. (2002) suggest conditions in the tropical southwest Pacific during the LIA were also consistently more saline than present. The most striking feature of the 420-year $\delta^{18}O$ record (Fig. 4B) is the abrupt 0.2‰ shift in $\delta^{18}O$ towards lower modern values between 1850 and 1870. With parallel Sr/Ca and $\delta^{18}O$ measurements, it is possible to remove the temperature component of the $\delta^{18}O$ record and show that over decade to century time scales the GBR coral $\delta^{18}O$ record is dominated by salinity variations. The 1870s shift, therefore, marks a significant freshening of GBR lagoon waters in the modern period. An equivalent 0.2‰ $\delta^{18}O$ shift is recorded 200 km offshore on the southern outer edge of the GBR (Druffel and Griffin, 1993), thus eliminating any local change in coastal runoff as a possible cause of the shift in $\delta^{18}O$. Furthermore, a synchronous late 19th century shift in $\delta^{18}O$ is also recorded at New Caledonia (Quinn et al., 1998) and Vanuatu (Quinn et al., 1993), and mirrored further afield in the eastern Pacific by the salinity-driven Gulf of Chiriquì $\delta^{18}O$ coral record (Linsley et al., 1994). Therefore, a process that influences seawater $\delta^{18}O$ throughout the southwest Pacific must be invoked to explain the spatial extent and timing of the shift in $\delta^{18}O$.

Globally, one of the most consistent features identified in historical and palaeoclimate records of the LIA is enhanced and highly variable atmospheric circulation (Grove, 1988; Crowley and North, 1991; Lamb, 1995; Kreutz et al., 1997). Palaeo-evidence for trade wind strength exists from the Peruvian Quelccaya ice core (14°S, 71°W; Thompson et al., 1986), which provides a high-resolution aeolian record of the Southern Hemisphere trade wind belt. During the LIA the number of large aeolian particles (diameter >1.59 µm) increased relative to the rest of the ice core, along with abrupt 20–30% shifts in microparticles and conductivities (Thompson et al., 1986). Hendy et al. (2002) proposed that higher salinities observed in the southwest Pacific coral between AD 1565 and 1870 (Fig. 4B) were the result of strengthened trade winds, increasing regional evaporation rates, and enhanced ocean advection. General circulation model experiments demonstrate that global climate responds to an exaggerated latitudinal temperature difference by intensifying large-scale atmospheric dynamics to maintain thermal balance, and that

the poleward transport of heat also increases through strengthened ocean circulation (Rind, 1998, 2000). Cooling and abrupt freshening of the tropical southwest Pacific after AD 1870 coincides with weakening of atmospheric circulation at the end of the LIA. At the same time, changes in surface-ocean circulation for the southwest Pacific, consistent with a reduction of the South Equatorial Current, are evident from abrupt shifts in GBR coral $\delta^{14}C$ (Druffel and Griffin, 1993, 1999) and Ba/Ca (E. Hendy, unpublished data).

More tropical palaeoclimate reconstructions will improve our understanding of the nature of the LIA and possible role of the tropics, however, two other issues are raised by these recent coral SST and SSS reconstructions. Firstly, because coral $\delta^{18}O$, the most frequently used coral climate-proxy tool, responds to a combination of SST and seawater $\delta^{18}O$ composition, it is critical that the contribution of salinity is resolved at all frequencies within the time scale of the record. For example, it has been proposed that salinity becomes proportionally more influential in a coral $\delta^{18}O$ record from New Caledonia at frequencies lower than interannual periods (Crowley et al., 1999) and yet this record, among other coral $\delta^{18}O$ records, has been included in multi-proxy temperature reconstructions (e.g., Jones et al., 1998; Mann et al., 1998). Secondly, it is necessary to replicate coral SST-reconstructions between coral colonies to confirm that climate signals are being faithfully recorded. Replication also highlights anomalous geochemical results due to secondary aragonite or skeletal abnormalities, which otherwise are unlikely to be identified, except by screening of the coral core by scanning electron microscopy (Müller et al., 2001; Hendy et al., 2002).

4. Holocene evolution of the El Niño-Southern oscillation

4.1. Modern ocean–atmosphere signature of ENSO

The ENSO phenomenon contributes a large portion of the interannual (2–7 years) variability in the modern climate system. Concerns about the future behaviour of ENSO under the influence of enhanced Greenhouse-gas forcing have led to renewed research into its long-term history to establish a baseline against which to understand modern ENSO variability. Investigating ENSO variability during the Holocene is particularly important because the effects of changes in background climate (temperature, orbital forcing of seasonal insolation, extra-tropical forcing) can be gauged without the complications of changing global ice cover and sea level (Markgraf and Diaz, 2000).

The IPWP is a region of critical importance for the development of ENSO events which, to a large degree, involve zonal displacements of the warm pool and the location of atmospheric convection. Today, the relatively warm, fresh, low-density water of the IPWP can be displaced easily by wind-driven currents associated with ENSO because the momentum is trapped in the shallow mixed layer (Picaut et al., 1996; Delcroix and Picaut, 1998). It is well known that warm pool water moves toward the central equatorial Pacific during El Niño events, together with the locus of atmospheric convection and rainfall (Rasmusson and Carpenter, 1982). The surface-ocean response of the tropical western Pacific to El Niño is a slight cooling of SSTs ($\sim 1^{\circ}C$), primarily due to the shallowing of the thermocline brought about by relaxation of the trade winds across the Pacific basin. The resulting re-arrangement of convective centres in the Walker Circulation brings lower than average rainfall to the IPWP region (Ropelewski and Halpert, 1987). A recent analysis of satellite estimates of oceanic precipitation and historical rain-gauge records provides the clearest picture yet of the pattern of ENSO-induced precipitation anomalies in the western Pacific region (Fig. 5; after Dai and Wigley, 2000).

Modern El Niño events show a marked tendency to peak toward the end of the calendar year (Tziperman et al., 1998) generally resulting in a diagnostic signal marked by initial cooling of SSTs in the tropical western Pacific, followed by lower than average rainfall. However, the ENSO cycle is not sinusoidal so La Niña is not simply the opposite of El Niño. While La Niña events generally bring higher than average rainfall to the tropical western Pacific, their locking to the annual cycle tends to be weak. Nevertheless, the tropical western Pacific is an excellent locality for reconstructing both the oceanic and atmospheric anomalies associated with ENSO.

Several sources of Holocene marine and terrestrial palaeoenvironmental records have recently provided new insights into the ENSO coupled ocean–atmosphere system in the tropical western Pacific region. In this section, we discuss terrestrial evidence (lacustrine, pollen, and charcoal records) for the timing of the onset of the modern ENSO. We then present a synthesis of mid-late Holocene coral records from the western and central Pacific, which are capable of recording individual ENSO events. The behaviour of ENSO teleconnections spanning the Little Ice Age to present is then examined using coral records from the Great Barrier Reef.

4.2. The terrestrial record of past ENSO events

4.2.1. Data

Charcoal preserved within lake and wetland sediments is a potential archive of regional fire episodes in the past associated with widespread and intense drought conditions experienced in the IPWP region during El

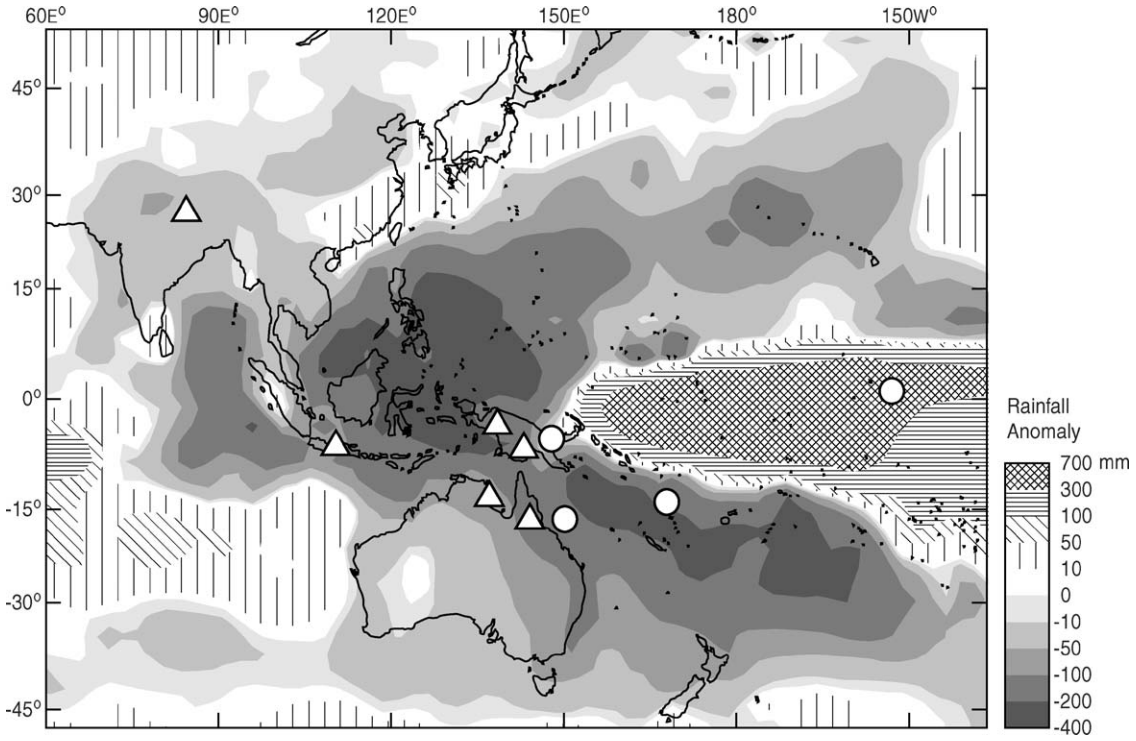

Fig. 5. Pattern of annual precipitation anomalies (mm) associated with moderate-strong El Niño events from 1900 to 1998. The data set is derived from historical rain-gauge records (1900–98) and satellite estimates of oceanic precipitation (1979–98). El Niño events are defined by periods exceeding 1.5 standard deviations for annual Darwin sea-level pressure (after Dai and Wigley, 2000). Locations of sites with palaeo-ENSO records discussed in text and Figs. 6–8 are shown by triangles (terrestrial records) and circles (coral records).

Niño events. In 1982–83 and 1997–98, severe drought and extensive fires occurred across large areas of island and mainland Southeast Asia and New Guinea in association with exceptionally strong El Niño conditions (Siegert et al., 2001). The environmental impact of these events was profound with extensive damage and destruction of vast tracks of normally wet tropical forest and failure of cultivated crops throughout the region. Such events should provide a clear ENSO signal in terrestrial sediment records.

The long-term record of century to millennial scale variability in charcoal abundance has been shown to closely correspond to predicted ENSO activity (Haberle et al., 2001; Haberle and Ledru, 2001). A composite charcoal abundance record derived from a combination of 10 lake and wetland records adjacent to the IPWP (Fig. 6) reflects changes in the pattern of regional burning from the LGM to the present. Despite the presence of humans in the region during the last 20,000 ^{14}C yr BP, there is no suggestion that fire frequencies were solely related to changing subsistence patterns of the human population. Two periods of high regional charcoal frequency are encountered, one during the post-glacial transition (17,000–9000 ^{14}C yr BP) and the second during the middle to late Holocene (5000 ^{14}C yr BP to the present). The higher charcoal concentrations are interpreted to reflect higher precipitation variability associated with ENSO. According to this model, the final onset of ENSO-like variability appears to have occurred $\sim$5000 ^{14}C yr BP.

A $\sim$5000–4000 year duration for the modern ENSO finds further support from geographically disparate sites showing increased vegetation disturbance across the Pacific basin (McGlone et al., 1992), Kalimantan (Anshari, 2000), island Melanesia (Haberle, 1996) and Australia (Shulmeister and Lees, 1995). In addition, several lakes in the Atherton Tablelands, northeastern Australia, have finely laminated bottom sediments spanning periods of up to several thousand years. These include Lake Barrine (laminae since 5000 ^{14}C yr BP; Walker and Owen, 1999) and Lake Eacham (bundles of laminae between 4000 and 2000 ^{14}C yr BP; Goodfield, 1983). In Lake Barrine, the laminae have been shown to accumulate at the average rate of one couplet per four years over the last 1000 years in association with periodic sediment turbulence during extremely cold winter conditions (Walker et al., 2000). While there has been no attempt to examine the role of ENSO in the lamination process, the appearance of laminae at a $\sim$4 year periodicity during the mid Holocene may point to the underlying onset of ENSO.

A similar picture for a mid-Holocene onset of modern ENSO periodicities is emerging for the tropical eastern Pacific (e.g., Sandweiss et al., 1996, 2001; Rodbell et al.,

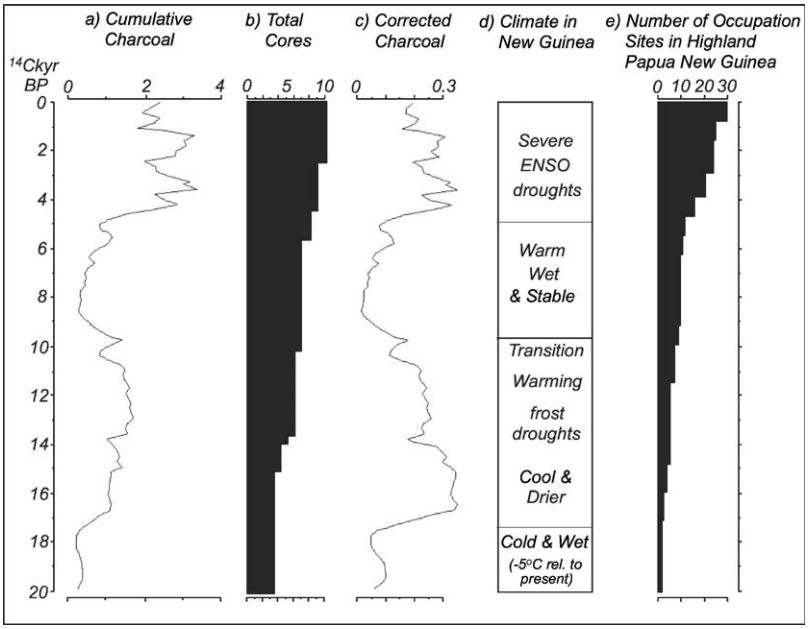

Fig. 6. (A) Composite charcoal record constructed by summing the 200 year values for 10 sites in Papua New Guinea and Indonesia plotted against age (^{14}C kyr BP); (B) number of cores with data for each 200 year period; (C) value in plot A divided by the corresponding value in plot B; (D) tentative summary of climate change in the highland Papua New Guinea region; and (E) number of human occupation sites from archaeological data in the highlands of Papua New Guinea as a measure of relative human influence (adapted from Fig. 2 in Haberle et al., 2001).

1999; Haug et al., 2001). A 15,000-year high-resolution record of storm-derived clastic sedimentation in Laguna Pallacocha, an alpine lake in Ecuador (Rodbell et al., 1999) provides a long, continuous record of high precipitation El Niño events. Spectral analysis of the record shows that the transition to modern ENSO periodicities (2–8.5 years) began ~7000–5000 ^{14}C yr BP. Highest El Niño frequencies occurred ~3500–2600 ^{14}C yr BP (Fig. 6). Analysis of mollusc assemblages from archaeological sites along the coast of Peru support the onset of ENSO at ~5800 ^{14}C yr BP and an increase in event frequency after 3200–2800 ^{14}C yr BP (Sandweiss et al., 1996, 2001). More indirect evidence of Holocene ENSO variability is provided by titanium concentrations in sediment from ODP site 1002 in the Cariaco Basin on the northern shelf of Venezuela (Haug et al., 2001). These display variations in runoff associated with shifts in the position of the Intertropical Convergence Zone (ITCZ). Once again, drier conditions ~5400 ^{14}C yr BP and enhanced runoff variability from 3800 to 2800 ^{14}C yr BP indicate a mean southward shift in the position of the ITCZ thought to be linked to mid-late Holocene changes in ENSO.

4.2.2. Models

Recent climate models for the early mid Holocene under altered insolation forcing suggest links between the strengthened Asian monsoon (e.g., Ganopolski et al., 1998), seasonally enhanced trade winds in the tropical Pacific, and the frequency and magnitude of strong El Niño temperature perturbations (Clement et al., 2000; Liu et al., 2000). When the coupled ocean–atmosphere climate models are forced with variations in the seasonal timing of equatorial heating, driven by precessional changes in the seasonal cycle of insolation, a steady increase in large El Niño events is observed during the Holocene, with a peak ~3000–1000 years ago (Fig. 7). In general, the palaeo-ENSO results agree with the model scenario. However, according to most of the palaeo-records, the onset of ENSO was more abrupt than predicted by the models, suggesting that factors other than insolation forcing may be at work.

4.3. High-resolution coral records of past ENSO events

High-resolution oxygen isotope (δ^{18}O) records from annually banded fossil *Porites* corals have been used successfully to investigate ENSO variability in the tropical Pacific during the Holocene. So far, coral δ^{18}O records with at least seasonal resolution have been published for the Great Barrier Reef (Gagan et al., 1997; Cane et al., 2000), Vanuatu (Corrège et al., 2000), Christmas (Kiritimati) Island (Woodroffe and Gagan, 2000; Woodroffe et al., 2003), and Papua New Guinea (Tudhope et al., 2001) (Fig. 4). Although individual coral records are restricted to time-slices spanning decades, they have the advantage of recording both changes in SST and salinity (precipitation) that can be attributed to single ENSO events.

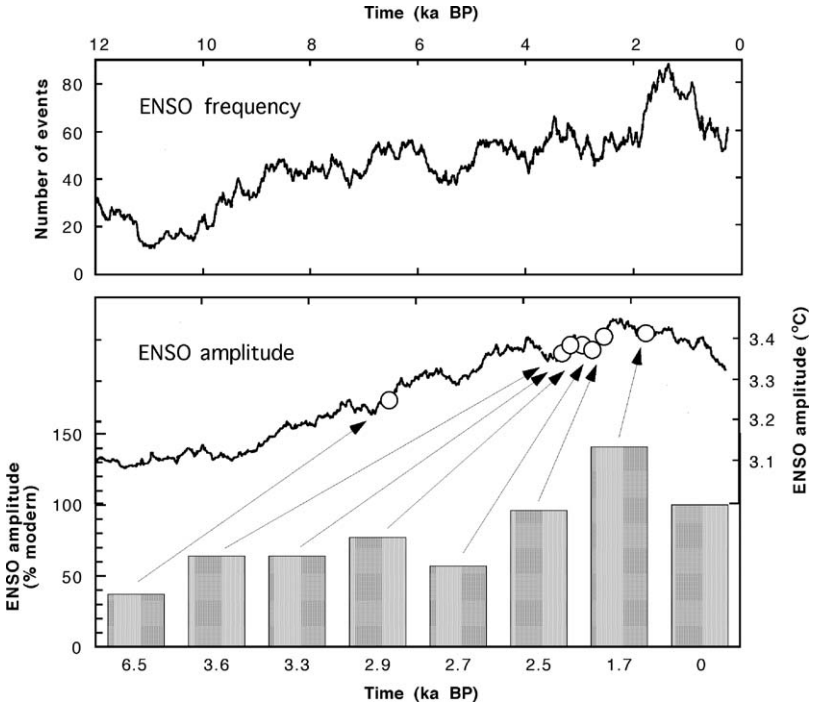

Fig. 7. Summary of reconstructed and insolation model estimates of the Holocene evolution of ENSO (calendar years before the present). (A) Solid curve shows modelled number of El Niño events defined as mean Dec-Feb SST anomalies exceeding 3°C in the NINO3 region of the eastern equatorial Pacific (5°N–5°S, 90°W–150°W) in 500 year overlapping windows (Clement et al., 2000). Stippled area shows proposed timing of onset of modern ENSO periodicities, based on available palaeoclimate reconstructions in the tropical Pacific region (see text). (B) Comparison of modelled amplitude of El Niño events with SST anomalies exceeding 3°C (Clement et al., 2000) and relative amplitude of $\delta^{18}O$ variability in the 2–7 year ENSO band for coral records from Huon Peninsula, Papua New Guinea (Tudhope et al., 2001) and Christmas (Kiritimati) Island, central equatorial Pacific (Woodroffe and Gagan, 2000; Woodroffe et al., 2003). Coral $\delta^{18}O$ variability has been scaled as a percentage of the modern (late 20th century) $\delta^{18}O$ variability at each site.

The ENSO signal in coral $\delta^{18}O$ records from the tropical western Pacific results from the combined effect on $\delta^{18}O$ of cooler SSTs and reduced input to the surface-ocean of ^{18}O-depleted rainfall during El Niño events (higher $\delta^{18}O$) and opposite effects during La Niñas (lower $\delta^{18}O$). Spectral analysis of a fossil coral $\delta^{18}O$ record spanning 49 years from the mid-Holocene (^{230}Th age: 6500 ± 70) of Papua New Guinea (Fig. 7B) shows that the magnitude of $\delta^{18}O$ variance in the 2–7 year ENSO band was ~60% weaker than 20th century values (Tudhope et al., 2001). New coral $\delta^{18}O$ records from fossil microatolls at Christmas Island record the migration of warm SSTs and convective rainfall into the central equatorial Pacific during El Niño events (Woodroffe and Gagan, 2000; Woodroffe et al., 2003). Three multi-decadal records from this locality indicate that ENSO amplitudes were 20–40% weaker than modern values during the period 3600–2900 ^{14}C yr BP. However, according to ENSO models (Clement et al., 2000; Liu et al., 2000), El Niño temperature anomalies in the mid-Holocene should have been no more than ~10% weaker than modern values (Fig. 7). Thus the ENSO variability given by the coral $\delta^{18}O$ records is surprisingly weak. Like the models, however, the coral records from both localities indicate that ENSO variability reached, or exceeded, modern values from 2500 to 1700 years ago.

The significant mismatch between the magnitude of combined SST and precipitation variability in the mid-Holocene, given by the coral $\delta^{18}O$ records, and the magnitude of El Niño SST variability, given by the models, suggests some degree of decoupling of ENSO ocean–atmosphere interactions. Coral Sr/Ca and U/Ca reconstructions of SST variability alone for the mid-Holocene tropical southwestern Pacific provide a different view of past ENSO variability. Reconstructed magnitudes of El Niño temperature perturbations at 4200 years ago, given by coral Sr/Ca and U/Ca palaeothermometry at Vanuatu, were larger than any observed in the modern record (Corrège et al., 2000). An investigation of the season-specific coupled ocean–atmosphere response of ENSO using coral Sr/Ca ratios in tandem with $\delta^{18}O$ for fossil corals growing in the Great Barrier Reef 6200 years ago yields a similar result (Gagan et al., 1997; Cane et al., 2000). Coupled measurements of Sr/Ca ratios and $\delta^{18}O$ values in corals provide a means for reconstructing the $\delta^{18}O$ of seawater, as well as temperature, by removal of the temperature component of the coral $\delta^{18}O$ signal (McCulloch et al., 1994; Gagan et al., 1998, 2000). In terms of El Niño

temperature perturbations, the mid-Holocene El Niño in the Great Barrier Reef was ~20% weaker than the relatively strong events from 1971 to 1992. In contrast, variability in summer precipitation in the mid-Holocene, as indicated by composites of coral $\delta^{18}O$, was ~70% weaker in the mid-Holocene, in agreement with coral $\delta^{18}O$ records from Papua New Guinea (Tudhope et al., 2001).

A full understanding of the palaeo-ENSO will require comparison of El Niño temperature forcing in the Pacific with rainfall perturbations that may be modulated under the influence of what is potentially an evolving ocean–atmosphere system. One possibility is that the Pacific Intertropical Convergence Zone (ITCZ) was located further north than at present during the mid-Holocene (Haug et al., 2001). At that time, interaction between the Southern Oscillation and ITCZ rainfall may have been weak, as indicated by unexpectedly low precipitation variability observed in terrestrial and coral palaeoclimate records from the Southern Hemisphere tropics. If the mean position of the ITCZ was located further north, the reduced ENSO variation in coral records from the mid-Holocene tropical Pacific may have been primarily temperature driven. In contrast, after ~3000 years ago tighter coupling in the Pacific between the more southerly ITCZ and the Southern Oscillation could serve to amplify ENSO precipitation variability and associated teleconnections. Such a scenario is consistent with terrestrial palaeoclimate records indicating a marked increase in El Niño activity ~3000 years ago.

These studies strongly support the continued development of a multi-proxy approach to reconstructing ENSO on long time scales. Coupling the emerging high-resolution terrestrial record of past ENSO events from tropical Southeast Asia and Australasia with exactly dated coral records from the IPWP region will be a fundamental step to developing a comprehensive history of ENSO variability and forcing over multiple spatial and temporal scales.

4.4. ENSO teleconnections over the past five centuries

4.4.1. Ice cores and tree rings

The historical record of major climatic perturbations linked to ENSO events in the IPWP region, including floods, cyclones and fires, is only beginning to be assessed (Grove and Chappell, 2000; Godley, 2002). Ice cores provide annual to millennial scale records of a range of proxies reflecting atmospheric conditions, including dust accumulation and $\delta^{18}O$ of snow fall, though most of the tropical records are currently limited to the past two millennia (Thompson et al., 2000a). On the more distal Tibetan Plateau, ice cores from Dasuopu have revealed annually laminated ice accumulation over at least the last 560 years (Thompson et al., 2000b), showing major fluctuations in dust concentrations and ice $\delta^{18}O$ associated with drought in the region. A number of major drought events recorded in the Dasuopu cores are concurrent with strong ENSO events, suggesting an association between ENSO and failure of the Asian monsoon. Continued work on these records will provide important comparative data for longer proxy records of ENSO activity and the extent of influence of ENSO in the Asia-Western Pacific region.

Tree-rings have the potential to provide annual and even seasonal data from which the long-term behaviour of ENSO may be derived. However, tree-ring analysis of tropical trees has been notoriously problematic due to a paucity of long-lived species and a lack of annual growth rings. One of the few exceptions to this is teak (*Tectona grandis*), with tree-rings that have been shown to be positively correlated with rainfall and the Southern Oscillation Index, as drought (or warm ENSO events) tends to produce poor growth in teak trees (Cook et al., 2000). Ongoing research by D'Arrigo et al. (1994) using teak has so far produced well-dated chronologies of around 500 years.

In locations more distal to the IPWP the potential has been explored for reconstructing ENSO with *Eucalyptus pauciflora* growing at high altitudes, *Callitris* in arid regions (Banks, 2000), and *Agathis* and *Araucaria* in the tropics of northern Australia (Ash, 1983). In New Zealand, the potential for producing long-term ENSO records from Kauri (*Agathis australis*) tree-ring chronologies has also been demonstrated by Fowler et al. (2000).

A recent tree-ring study by Stahle et al. (1998) has successfully exploited ENSO teleconnection patterns to reconstruct winter (March–October) Southern Oscillation Index (SOI) variability since AD 1706. The proxy data set comprises 20 sub-tropical tree-ring chronologies from the southern United States and Mexico, and a single tropical teak chronology from Java (D'Arrigo et al., 1994). Surprisingly, the correlation of the Javan teak chronology with the SOI is weaker than that for the other sub-tropical records, despite its location on the western end of the Southern Oscillation. The most notable feature of the record is a marked increase in the frequency of strong ENSO events after 1880. Comparisons with coral SST and rainfall reconstructions from the tropical Pacific (Cole et al., 1993; Dunbar et al., 1994) and Peruvian ice core records (Thompson et al., 1984) suggest that the strengthening of ENSO after 1880 reflects a change in the ENSO system, and not simply an enhancement of ENSO teleconnections.

4.4.2. Corals

The strength and significance of correlations, or teleconnections, between ENSO events and the resulting near-global climate anomalies are known to have varied during the 20th century (e.g., Elliott and Angell, 1988;

Allan et al., 1996; Allan, 2000; Mann et al., 2000a; Cai et al., 2001). Over the period of instrumental records, links between climatic anomalies in ENSO-sensitive regions and ENSO indices were stronger prior to the 1920s and after the 1960s, but weakened dramatically between 1920 and 1950. This latter period was associated with weaker ENSO activity, and reduced interannual rainfall variability in Australia (Allan et al., 1996). Typically, El Niño years correspond with reduced summer monsoon rainfall over northeast Australia and the GBR region. The opposite occurs in La Niña years when the summer monsoon circulation tends to be more vigorous leading to above average rainfall and river flow into the GBR, lowering salinity and increasing the turbidity of reef waters (Lough, 2001).

Terrestrial runoff can be reconstructed from the luminescent (or 'fluorescent') bands in the skeleton of massive *Porites* coral, which are visible under long-wave UV light (Isdale, 1984). The timing, width and intensity of the luminescent lines in corals from the central GBR are closely related to the timing and intensity of runoff from Queensland's largest river, the Burdekin (Isdale, 1984; Isdale et al., 1998), and Queensland summer monsoonal rainfall (Lough, 1991). The climate in the GBR is dominated by a winter dry season and a summer wet season (October–March) when up to 70% of annual rainfall occurs (Lough, 1994, 2001). Long periods of low flow during the dry season contrast dramatically with high river flows in January–March, when, typically, 1–3 strong flows lasting only a few days contribute the bulk of the annual discharge (Lough, 1994). Interannual variability of river run-off and rainfall is dramatic; Burdekin River discharge in 1974 was over 750% of median annual flow for the period 1922–1992, compared with a low of 5% of median annual flow in 1931. This high interannual variability is linked to ENSO events.

In a recent study, eight multi-century coral cores were used to develop a 373-year time series of annual luminescence (Hendy et al., 2003). Following methods adapted from dendrochronology, skeleton-plots of annual luminescent banding were produced for each core with events both positive (strong luminescence) and negative (absence of luminescence) ranked according to intensity. Characteristic patterns of distinct luminescent lines were cross-dated and a single master chronology was constructed back to AD 1615 (Fig. 8A). In addition to improving dating control, the luminescence master chronology is a proxy record for freshwater runoff to the GBR and correlates significantly with regional rainfall ($r = 0.65$, 1891–1985; Queensland summer rainfall, (Lough, 1997)) and river discharge records ($r = 0.84$, 1923–1985). The luminescence master also provides insights into the variability of ENSO teleconnection patterns over the past several centuries.

The varying strength of ENSO teleconnections can be seen in the moving correlation between the luminescence master and instrumental SOI (Fig. 8C; dotted line). As found for Queensland rainfall (Lough, 1991; Lough, 1997; Cai et al., 2001), correlations between the river runoff proxy and the SOI are significant prior to ~1920 and after ~1960, but break down in the intervening period ~1920–1950. This instability in the strength of ENSO teleconnections means that the luminescence master chronology is not a particularly strong measure of ENSO. In combination with other proxy climate series, however, the luminescence master provides a

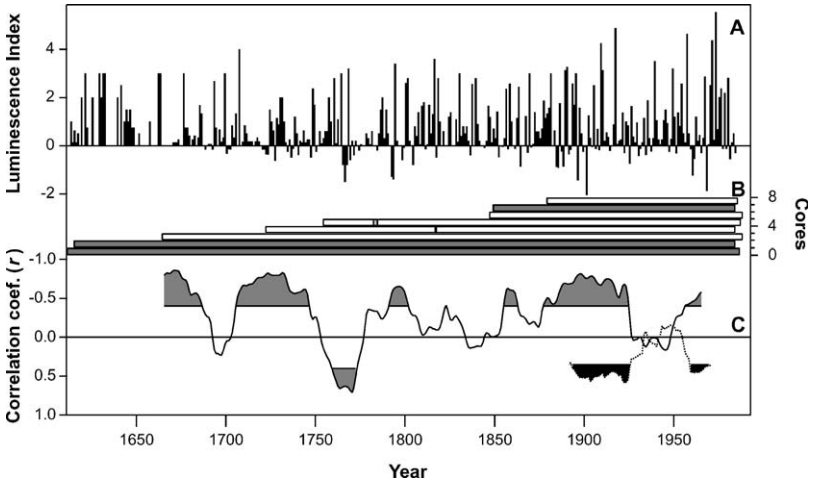

Fig. 8. Standardised UV luminescence master series for the central GBR for AD 1615–1985 (after Hendy et al., 2003) (A) The number of *Porites* coral cores contributing to the study through time (B) are shown with those from midshelf colonies shaded dark grey. The distinction between midshelf and inshore cores is important because inshore cores are more sensitive recorders of negative events (droughts). In the early part of the chronology, such events are absent when inshore cores are not present to contribute to the master chronology. Cross correlations (C) for a 30-year sliding window between the luminescence master series, the summer SOI (dotted line and black shading), and the NINO3 Mann et al. (2000b) SST reconstruction (solid line and grey shading). NINO3 data (1650–1980 AD) are from ftp://eclogite.geo.umass.edu/pub/mann/MANETAL98/nino3.dat. The NINO3 series has been smoothed with a 5-year Gaussian filter. Significance of correlations at 0.05 level is indicated by shading.

record of the fluctuations in strength of ENSO teleconnections with northeast Australian climate.

The strength of the correlation between the luminescence master series and a multi-proxy reconstruction of the NINO3 SST index (5°S–5°N, 90°W–150°W) of Mann et al. (2000b) varies through time (Fig. 8C). Significant negative correlations between the two series mimic the periods of fluctuating teleconnection strength during the 20th century, such as the significant teleconnection between the late 1870s and 1920s. Earlier periods of significant correlation with the NINO3 series occur from the mid-17th to late 18th centuries, suggesting that ENSO-related teleconnections were as dominant then as in recent decades.

Disappearance of the signal for most of the period from the 1800s to 1870s suggests that ENSO-teleconnections with Queensland rainfall were not operating for much of the 19th century. During this period both interdecadal and interannual variability are suppressed and climatic conditions were possibly analogous to the 1920s–50s. Reduced variability during the 19th century is also reported in corals from the NINO3 region (Dunbar et al., 1994) and the central equatorial Pacific (Urban et al., 2000). Variability in tree-ring series from North America and Java (Stahle et al., 1998) is also interpreted as reduced ENSO activity and/or weaker ENSO teleconnections, which is supported by evidence for shifts in teleconnection patterns over North America (Cole and Cook, 1998). The recent increase in ENSO variability and the strength of ENSO teleconnections are, therefore, not confined to the last century. This low-frequency mode of natural climate variability needs to be understood and incorporated into global climate models.

5. Conclusions and future directions

This review highlights the following recent advances in our knowledge of the temperature, size, and variability of the IPWP and the nature of the ENSO since the LGM:

- SSTs in the IPWP during the LGM were ~3°C cooler than at present. In the central portion of the IPWP, the rapid post-glacial rise in SST led the deglaciation by ~3000 years to produce near-modern SSTs by the early Holocene. In contrast, further west and north, post-glacial shifts in SSTs in the South China and Sulu Seas were synchronous with abrupt climate changes in the North Atlantic.
- Palaeo-ENSO records throughout the tropical Pacific region identify the onset of modern ENSO periodicities ~5000 years ago, followed by an abrupt increase in ENSO magnitude ~3000 years ago. Individual ENSO events recorded by corals reveal that the precipitation response to El Niño temperature anomalies was subdued in the mid-Holocene. The apparent non-linear onset of ENSO in the late Holocene appears to reflect abruptly enhanced interaction between the Southern Oscillation and the Pacific Intertropical Convergence Zone.
- A 420-year coral record of Sr/Ca and $\delta^{18}O$ from the Great Barrier Reef, Australia identifies a dramatic shift in the tropical ocean–atmosphere system which occurred at the end of the Little Ice Age, possibly in response to a reduction in latitudinal temperature gradients. Comparisons of precipitation variability recorded by Great Barrier Reef corals with ENSO indices for the last 350 years confirm non-stationarity of ENSO teleconnections is a natural characteristic of recent climate.

Future advances in understanding the role of the IPWP in global climate and the history of ENSO will require new palaeoclimate reconstructions. A wide range of palaeoclimate sources have now been developed and, with increased spatial and temporal coverage, it should be possible to clarify changes in zonal and meridional temperature gradients and the displacement of centres of atmospheric convection through time. For example, coupling the emerging high-resolution terrestrial record of past ENSO events from tropical Southeast Asia and Australasia with exactly dated coral records from the IPWP region will be a fundamental step towards the development of a comprehensive history of ENSO variability and forcing over multiple time scales. Comparisons of climate models and palaeoclimate data will provide valuable tests of theories to explain past climate variability and insights relevant to understanding the processes of climate change under the influence of enhanced greenhouse gas forcing.

Acknowledgements

We thank the IGBP-PAGES for sponsoring the Pole-Equator-Pole Transect II initiative data synthesis meeting, which provided the impetus for this review paper. We are grateful to Peter Isdale and David Hopley for providing access to their exquisite suite of Great Barrier Reef coral cores. Special thanks are given to Bambang Suwargadi, Dudi Prayudi, and Anto Sanyoto of the Indonesian Institute of Sciences for dedicated assistance during fossil coral drilling expeditions to Sumba and Alor. Particular thanks go to Joe Cali, Graham Mortimer, and Heather Scott-Gagan for skilful mass spectrometry in the RSES laboratories. The collaborative contributions of Linda Ayliffe, Janice Lough, Heather Scott-Gagan, Chantal Alibert, and Malcolm McCulloch to the coral records reviewed in this paper are greatly appreciated. Janice Lough and David Stahle

provided constructive reviews of the manuscript. Support for the authors' research in the Great Barrier Reef, Indonesia, and Papua New Guinea was provided by the Australian National University, The Australian Institute of Marine Science, The Indonesian Institute of Sciences, and Monash University.

References

Alibert, C., McCulloch, M.T., 1997. Strontium/calcium ratios in modern *Porites* corals from the Great Barrier Reef as a proxy for sea surface temperature: calibration of the thermometer and monitoring of ENSO. Paleoceanography 12, 345–365.

Allan, R.J., 2000. ENSO and climatic variability in the past 150 years. In: Diaz, H.F., Markgraf, V. (Eds.), El Niño and the Southern Oscillation: Multiscale Variability and Global and Regional Impacts. Cambridge University Press, Cambridge, pp. 3–55.

Allan, R.J., Lindesay, J., Parker, D., 1996. El Niño Southern Oscillation and Climate Variability. CSIRO Publishing, Collingwood, Australia, 405pp.

Anshari, G., 2000. Late Quaternary Vegetation and Environments in the Lake Sentarum Wildlife Reserve, West Kalimantan, Indonesia. Ph.D. Thesis. School of Geography and Environmental Science, Monash University, Australia, 292pp, unpublished.

Ash, J., 1983. Growth rings in *Agathis robusta* and *Araucaria cunninghamii* from tropical Australia. Australian Journal of Botany 34, 197–205.

Banks, J.C.G., 2000. El Niño and the Australian climate: the dendrochronological potential of Australian trees for dating climate extremes of drought, fire and flood. In: Grove, R.H., Chappell, J. (Eds.), El Niño: History and Crisis. The White Horse Press, Cambridge, pp. 224–230.

Beck, J.W., Edwards, R.L., Ito, E., Taylor, F.W., Récy, J., Rougerie, F., Joannot, P., Henin, C., 1992. Sea-surface temperature from coral skeletal strontium/calcium ratios. Science 257, 644–647.

Beck, J.W., Récy, J., Taylor, F., Edwards, R.L., Cabioch, G., 1997. Abrupt changes in early Holocene tropical sea surface temperature derived from coral records. Nature 385, 705–707.

Bradley, R.S., 2000. Past global changes and their significance for the future. Quaternary Science Reviews 19, 391–402.

Bradley, R.S., Jones, P.D., 1993. Little Ice Age summer temperature variations: their nature and relevance to recent global warming trends. The Holocene 3, 367–376.

Cai, W., Whetton, P.H., Pittock, A.B., 2001. Fluctuations of the relationship between ENSO and northeast Australian rainfall. Climate Dynamics 17, 421–432.

Cane, M.R., Clement, A.C., 1999. A role for the tropical Pacific coupled ocean–atmosphere system on Milankovitch and Millennial timescales: Part II: global impacts. mechanisms of global climate change at millennial time scales. Geophysical Monograph 112, 373–383.

Cane, M.R., Clement, A.C., Gagan, M.K., Ayliffe, L.K., Tudhope, A.W., 2000. ENSO through the Holocene as depicted in corals and a model simulation. In: Gould, J., Villwock, A. (Eds.), International Geosphere-Biosphere Program (PAGES) 8(1), 3–7.

Clement, A., Cane, M., Seager, R., 2001. An orbitally driven tropical source for abrupt climate change. Journal of Climate 14, 2369–2375.

Clement, A.C., Seager, R., Cane, M.A., 2000. Suppression of El Niño during the mid-Holocene by changes in the Earth's orbit. Paleoceanography 15, 731–737.

CLIMAP Members, 1981. The surface of the Ice Age Earth. Science 191, 1131–1137.

Cohen, A.L., Layne, G.D., Hart, S.R., 2001. Kinetic control of skeletal Sr/Ca in a symbiotic coral: implications for the paleotemperature proxy. Paleoceanography 16, 20–26.

Cole, J.E., Cook, E.R., 1998. The changing relationship between ENSO variability and moisture balance in the continental United States. Geophysical Research Letters 25, 4529–4532.

Cole, J.E., Fairbanks, R.G., Shen, G.T., 1993. Recent variability in the Southern Oscillation: isotopic results from a Tarawa Atoll coral. Science 260, 1790–1793.

Cook, E.R., D'Arrigo, R.D., Cole, J.E., Stahle, D.W., Villalba, R., 2000. Tree-ring records of past ENSO variability and forcing. In: Diaz, H.F., Markgraf, V. (Eds.), El Niño and the Southern Oscillation: Multiscale Variability and Global and Regional Impacts. Cambridge University Press, Cambridge, pp. 297–324.

Correge, T., Delcroix, T., Recy, J., Beck, W., Cabioch, G., Le Cornec, F., 2000. Evidence for stronger El Niño-Southern Oscillation (ENSO) events in a mid-Holocene massive coral. Paleoceanography 14, 465–470.

Correge, T., Quinn, T., Delcroix, T., Le Cornec, F., Récy, J., Cabioch, G., 2001. Little Ice Age sea surface temperature variability in the southwest tropical Pacific. Geophysical Research Letters 28, 3477–3480.

Crowley, T.J., 2000. Causes of climate change over the past 1000 years. Science 289, 270–277.

Crowley, T.J., North, G.R., 1991. Paleoclimatology. Oxford University Press, New York.

Crowley, T.J., Quinn, T.M., Hyde, W.T., 1999. Validation of coral temperature calibrations. Paleoceanography 14, 605–615.

Dai, A., Wigley, T.M.L., 2000. Global patterns of ENSO-induced precipitation. Geophysical Research Letters 27, 1283–1286.

D'Arrigo, R.D., Jacoby, G.C., Krusic, P.J., 1994. Progress in dendroclimatic studies in Indonesia. Terrestrial, Atmospheric and Oceanographic Sciences 5, 349–363.

Delcroix, T., Picaut, J., 1998. Zonal displacement of the western equatorial Pacific "fresh pool". Journal of Geophysical Research 103, 1087–1098.

deVilliers, S., Shen, G.T., Nelson, B.K., 1994. The Sr/Ca-temperature relationship in coralline aragonite: influence of variability in (Sr/Ca) seawater and skeletal growth parameters. Geochimica et Cosmochimica Acta 58, 197–208.

Druffel, E.R.M., Griffin, S., 1993. Large variations of surface ocean radiocarbon: evidence of circulation changes in the southwestern Pacific. Journal of Geophysical Research 98, 20249–20259.

Druffel, E.R.M., Griffin, S., 1999. Variability of surface ocean radiocarbon and stable isotopes in the southwestern Pacific. Journal of Geophysical Research—Oceans 104, 23607–23613.

Dunbar, R.B., Wellington, G.M., Colgan, M.W., Glynn, P.W., 1994. Eastern Pacific sea surface temperature since 1600 A.D: the $\delta^{18}O$ record of climate variability in galápagos corals. Paleoceanography 9, 291–315.

Edwards, R.L., Chen, J.H., Wasserburg, G.J., 1987. ^{238}U–^{234}Th–^{230}Th–^{232}Th Systematics and the precise measurement of time over the past 500,000 years. Earth and Planetary Science Letters 81, 175–192.

Elliott, W.P., Angell, J.K., 1988. Evidence for changes in Southern Oscillation relationships during the last 100 years. Journal of Climate 1, 729–737.

Fowler, A., Palmer, J., Salinger, J., Ogden, J., 2000. Dendroclimatic interpretation of tree-rings in *Agathis australis* (kauri): 2. evidence of a significant relationship with ENSO. Journal of the Royal Society of New Zealand 30, 277–292.

Gagan, M.K., Ayliffe, L.K., Anker, S., Hopley, D., McCulloch, M.T., Isdale, P.J., Chappell, J., Head, M.J., 1997. Great Barrier Reef 'Climatic Optimum' at 5800 yBP. In: Oldfield, F. (Ed.), International Geosphere-Biosphere Program (PAGES) Newsletter, 5(1), 15–16.

Gagan, M.K., Ayliffe, L.K., Hopley, D., Cali, J.A., Mortimer, G.E., Chappell, J., McCulloch, M.T., Head, M.J., 1998. Temperature and surface-ocean water balance of the mid-Holocene tropical western Pacific. Science 279, 1014–1018.

Gagan, M.K., Ayliffe, L.K., Beck, J.W., Cole, J.E., Druffel, E.R.M., Dunbar, R.B., Schrag, D.P., 2000. New views of tropical paleoclimates from corals. Quaternary Science Reviews 19, 45–64.

Ganopolski, A., Kubatzki, C., Claussen, M., Brovkin, V., Petoukhov, V., 1998. The influence of vegetation-atmosphere-ocean interaction on climate during the mid-Holocene. Science 280, 1916–1919.

Godley, D., 2002. The reconstruction of flood regimes in SE Asia from El Niño-Southern Oscillation (ENSO) related records. In: Kershaw, A.P., David, B., Tapper, N., Penny, D., Brown, J. (Eds.), Bridging Wallace's Line: The Environmental and Cultural History and Dynamics of the SE Asian-Australasian Region. Catena Verlag, Reiskirchen, pp. 229–254.

Goodfield, M.L., 1983. A Holocene pollen analytical study of Lake Eacham, Atherton Tableland, north-east Queensland. B.Sc. Honours Thesis, Department of Geography, Monash University, 146pp, unpublished.

Grove, J.M., 1988. The Little Ice Age. Methuen & Co Ltd, London.

Grove, R.H., Chappell, J., 2000. El Niño chronology and the history of global crises during the Little Ice Age. In: Grove, R.H., Chappell, J. (Eds.), El Niño: History and Crisis. The White Horse Press, Cambridge, pp. 5–34.

Haberle, S.G., 1996. Explanations for palaeoecological changes on the northern plains of Guadalcanal, Solomon Islands: the last 3200 years. The Holocene 6, 333–338.

Haberle, S.G., Ledru, M.-P., 2001. Correlations among charcoal records of fires from the past 16,000 years in Indonesia, Papua New Guinea, and Central and South America. Quaternary Research 55, 97–104.

Haberle, S.G., Hope, G.S., van der Kaars, S., 2001. Biomass burning in Indonesia and Papua New Guinea: natural and human induced fire events in the fossil record. Palaeogeography, Palaeoclimatology, Palaeoecology 171, 259–268.

Hantoro, W.S., Pirazzoli, P.A., Jouannic, C., Faure, H., Hoang, C.T., Radtke, U., Causse, C., Borel Best, M., Lafont, R., Bieda, S., Lambeck, K., 1994. Quaternary uplifted coral terraces on Alor Island, east Indonesia. Coral Reefs 13, 215–223.

Haug, G.H., Hughen, K.A., Sigman, D.M., Peterson, L.C., Rohl, U., 2001. Southward migration of the intertropical convergence zone through the Holocene. Science 293, 1304–1308.

Hendy, E.J., Gagan, M.K., Alibert, C., McCulloch, M.T., Lough, J.M., Isdale, P.J., 2002. Abrupt shift in tropical sea surface salinity at end of Little Ice Age. Science 295, 1511–1514.

Hendy, E.J., Gagan, M.K., Lough, J.M., 2003. Chronological control of coral records using luminescent lines and evidence for non-stationary ENSO teleconnections in northeast Australia. The Holocene 13, 187–199.

Imbrie, J., Hays, J.D., Martinson, D.G., McIntyre, A., Mix, A.C., Morley, J.J., Pisias, N.G., Prell, W.L., Shackleton, N.J., 1984. The orbital theory of Pleistocene climate: support from a revised chronology of the marine ^{18}O record. In: Berger, A.L., Imbrie, J., Hays, J., Kukla, G., Saltzman, B. (Eds.), Milankovitch and Climate: Understanding the Response to Astronomical Forcing. Dordrecht:Reidel, Netherlands, pp. 269–305.

Isdale, P., 1984. Fluorescent bands in massive corals record centuries of coastal rainfall. Nature 310, 578–579.

Isdale, P.J., Stewart, B.J., Tickle, K.S., Lough, J.M., 1998. Palaeohydrological variation in a tropical river catchment: a reconstruction using fluorescent bands in corals of the Great Barrier Reef, Australia. The Holocene 8, 1–8.

Jones, P.D., Briffa, K.R., Barnett, T.P., Tett, S.F.B., 1998. High-resolution palaeoclimatic records for the last millennium: interpretation, integration and comparison with general circulation model control-run temperatures. The Holocene 8, 455–471.

Jones, P.D., Osborn, T.J., Briffa, K.R., 2001. The evolution of climate over the last millennium. Science 292, 662–667.

Kienast, M., Steinke, S., Stattegger, K., Calvert, S.E., 2001. Synchronous tropical south China Sea SST change and Greenland warming during deglaciation. Science 291, 2132–2134.

Kreutz, K.J., Mayewski, P.A., Meeker, L.D., Twicker, M.S., Whitlow, S.I., Pittalwala, I.I., 1997. Bipolar changes in atmospheric circulation during the Little Ice Age. Science 277, 1294–1296.

Kudrass, H.R., Erlenkueser, H., Vollbrecht, R., Weiss, W., 1991. Global nature of the Younger Dryas cooling event inferred from oxygen isotope data from Sulu Sea cores. Nature 349, 406–409.

Lamb, H.H., 1995. Climate, History and the Modern World. Routledge, London, pp. 433.

Lau, K.-M., Chan, P.H., 1982. Intraseasonal and interannual variations of tropical convection: a possible link between the 40-day mode and ENSO. Journal of Atmospheric Science 45, 950–972.

Lea, D.W., Mashiotta, T.A., Spero, H.J., 1999. Controls on magnesium and strontium uptake in planktonic foraminifera determined by live culturing. Geochimica et Cosmochimica Acta 63, 2369–2379.

Lea, D.W., Pak, D.K., Spero, H.J., 2000. Climate impact of late Quaternary equatorial Pacific sea surface temperature variations. Science 289, 1719–1724.

Linsley, B.K., 1996. Oxygen-isotope record of sea level and climate variations in the Sulu Sea over the past 150,000 years. Nature 380, 234–237.

Linsley, B.K., Thunell, R.C., 1990. The record of deglaciation in the Sulu Sea: evidence for the Younger Dryas in the western Pacific. Paleoceanography 5, 1025–1039.

Linsley, B.K., Dunbar, R.B., Wellington, G., Mucciarone, D.A., 1994. A coral-based reconstruction of intertropical convergence zone variability over Central America since 1707. Journal of Geophysical Research 99, 9977–9994.

Linsley, B.K., Wellington, G.M., Schrag, D.P., 2000. Decadal sea surface temperature variability in the subtropical south pacific from 1726 to 1997 A.D. Science 290, 1145–1148.

Liu, Z., Kutzbach, J., Wu, L., 2000. Modeling climate shift of El Niño variability in the Holocene. Geophysical Research Letters 27, 2265–2268.

Lough, J.M., 1991. Rainfall variations in Queensland, Australia: 1891–1986. International Journal of Climatology 11, 745–768.

Lough, J.M., 1994. Climate variation and El Niño-Southern Oscillation events on the Great Barrier Reef: 1958 to 1987. Coral Reefs 13, 181–195.

Lough, J.M., 1997. Regional indices of climate variation: temperature and rainfall in Queensland, Australia. International Journal of Climatology 17, 55–66.

Lough, J.M., 2001. Climate variability and change on the Great Barrier Reef. In: Wolanski, E. (Ed.), Oceanographic Processes on Coral Reefs: Physics–Biology Links in the Great Barrier Reef. CRC Press, Boca Raton, FL, pp. 269–300.

Mann, M.E., Bradley, R.S., Hughes, M.K., 1998. Global-scale temperature patterns and climate forcing over the past six centuries. Nature 392, 779–787.

Mann, M.E., Bradley, R.S., Hughes, M.K., 1999. Northern Hemisphere temperatures during the past millennium: inferences, uncertainties, and limitations. Geophysical Research Letters 26, 759–762.

Mann, M.E., Bradley, R.S., Hughes, M.K., 2000a. Long-term variability in the El Niño/Southern oscillation and associated teleconnections. In: Diaz, H.F., Markgraf, V. (Eds.), El Niño and the Southern Oscillation: Multiscale Variability and Global and Regional Impacts. Cambridge University Press, Cambridge, pp. 357–412.

Mann, M.E., Gille, E., Overpeck, J., Gross, W., Bradley, R.S., Keimig, F.T., Hughes, M.K., 2000b. Global temperature patterns in past centuries: an interactive presentation. Earth Interactions 4, 1–29.

Markgraf, V., Diaz, H.F., 2000. The past ENSO record: a synthesis. In: Diaz, H.F., Markgraf, V. (Eds.), El Niño and the Southern Oscillation: Multiscale Variability and Global and Regional Impacts. Cambridge University Press, Cambridge, pp. 465–488.

McCulloch, M.T., Gagan, M.K., Mortimer, G.E., Chivas, A.R., Isdale, P.J., 1994. A high-resolution Sr/Ca and $\delta^{18}O$ coral record from the Great Barrier Reef, Australia, and the 1982–1983 El Niño. Geochimica et Cosmochimica Acta 58, 2747–2754.

McCulloch, M.T., Mortimer, G., Esat, T., Xianhua, L., Pillans, B., Chappell, J., 1996. High resolution windows into early Holocene climate: Sr/Ca coral records from the Huon Peninsula. Earth and Planetary Science Letters 138, 169–178.

McGlone, M.S., Kershaw, A.P., Markgraf, V., 1992. El Niño/Southern Oscillation climatic variability in Australasian and South American palaeoenvironmental records. In: Diaz, H.F., Markgraf, V. (Eds.), El Niño: Historical and Palaeoclimatic Aspects of the Southern Oscillation. Cambridge University Press, Cambridge, pp. 435–462.

McGregor, H.V., Gagan, M.K., 2003. Diagenesis, geochemistry of Porites corals from Papua New Guinea: Implications for paleoclimate reconstruction. Geochimica et Cosmochimica Acta 67, 2147–2156.

Müller, A., Gagan, M.K., McCulloch, M.T., 2001. Early marine diagenesis in corals and geochemical consequences for paleoceanographic reconstructions. Geophysical Research Letters 28, 4471–4474.

Oberhuber, J.M., 1988. An atlas based on the COADS data set: The budgets of heat, buoyancy and turbulent kinetic energy at the surface of the global ocean. Rep. 15. Max-Planck Inst., Hamburg, Germany, 20pp.

Ohkouchi, N., Kawamura, K., Nakamura, T., Taira, A., 1994. Small changes in the sea surface temperature during the last 20,000 years: molecular evidence from the western tropical Pacific. Geophysical Research Letters 21, 2207–2210.

Pelejero, C., Grimalt, J.O., 1999. The correlation between the U^k_{37} index and sea surface temperatures in the warm boundary: the South China Sea. Geochimica et Cosmochimica Acta 61, 4789–4797.

Pelejero, C., Grimalt, J.O., Heilig, S., Kienast, M., Wang, L., 1999. High-resolution U^k_{37} temperature reconstructions in the South China Sea over the past 220 kyr. Paleoceanography 14, 24–231.

Picaut, J., Ioualalen, M., Menkes, C., Delcroix, T., McPhaden, M.J., 1996. Mechanism of the zonal displacements of the Pacific Warm Pool: implications for ENSO. Science 274, 1486–1489.

Pirazzoli, P.A., Radtke, U., Hantoro, W.S., Jouannic, C., Hoang, C.T., Causse, C., Borel Best, M., 1991. Quaternary raised coral-reef terraces on Sumba Island, Indonesia. Science 252, 1834–1836.

Quinn, T.M., Taylor, F.W., Crowley, T.J., 1993. A 173 year stable isotope record from a tropical south pacific coral. Quaternary Science Reviews 12, 407–418.

Quinn, T.M., Crowley, T.J., Taylor, F.W., Henin, C., Joannot, P., Join, Y., 1998. A multicentury stable isotope record from a New Caledonia coral: interannual and decadal sea surface temperature variability in the southwest Pacific since 1657 A.D. Paleoceanography 13, 412–426.

Ramanathan, V., Collins, W., 1991. Thermodynamic regulation of ocean warming by cirrus clouds deduced from observations of the 1987 El Niño. Nature 351, 27–32.

Rasmusson, E.M., Carpenter, T.H., 1982. Variations in tropical sea surface temperature and surface wind fields associated with the El Niño/Southern Oscillation. Monthly Weather Review 110, 354–384.

Rind, D., 1998. Latitudinal temperature gradients and climate change. Journal of Geophysical Research 103, 5943–5971.

Rind, D., 2000. Relating paleoclimate data and past temperature gradients: some suggestive rules. Quaternary Science Reviews 19, 381–390.

Rodbell, D.T., Seltzer, G.O., Anderson, D.M., Abbott, M.B., Enfield, D.B., Newman, J.H., 1999. An ~15,000-year record of El Niño-driven alluviation in southwestern Ecuador. Science 283, 516–520.

Ropelewski, C.F., Halpert, M.S., 1987. Global and regional scale precipitation patterns associated with the El Niño/Southern Oscillation. Monthly Weather Review 115, 1606–1626.

Sandweiss, D.H., Richardson III, J.B., Reitz, E.J., Rollins, H.B., Maasch, K.A., 1996. Geoarchaeological evidence from Peru for a 5000 B.P. onset of El Niño. Science 273, 1531–1533.

Sandweiss, D.H., Maasch, K.A., Burger, R.L., Richardson, J.B., Rollins, H.B., Clement, A., 2001. Variation in Holocene El Niño frequencies: climate records and cultural consequences in ancient Peru. Geology 29, 603–606.

Shulmeister, J., Lees, B.G., 1995. Pollen evidence from tropical Australia for the onset of an ENSO-dominated climate at c. 4000 BP. The Holocene 5, 10–18.

Siegert, F., Ruecker, G., Hinrichs, A., Hoffmann, A.A., 2001. Increased damage from fires in logged forests during droughts caused by El Niño. Nature 414, 437–440.

Stahle, D.W., D'Arrigo, R.D., Krusic, P.J., Cleaveland, M.K., Cook, E.R., Allan, R.J., Cole, J.E., Dunbar, R.B., Therrell, M.D., Gay, D.A., Moore, M.D., Stokes, M.A., Burns, B.T., Villanueva-Diaz, J., Thompson, L.G., 1998. Experimental dendroclimatic reconstruction of the Southern Oscillation. Bulletin of the American Meteorological Society 79, 2137–2152.

Stoll, H.M., Schrag, D.P., 1998. Effects of Quaternary sea level cycles on strontium in seawater. Geochimica et Cosmochimica Acta 62, 1107–1118.

Stott, L., Poulsen, C., Lund, S., Thunell, R., 2002. Super ENSO and global climate oscillations at millennial time scales. Science 297, 222–226.

Stuiver, M., Reimer, P.J., 1993. Extended ^{14}C data base and revised CALIB 3.0 ^{14}C age calibration program. Radiocarbon 35, 215–230.

Thompson, L.G., Mosley-Thompson, E., Arnao, B.M., 1984. El Niño-Southern Oscillation events recorded in the stratigraphy of the tropical Quelccaya ice cap, Peru. Science 226, 50–53.

Thompson, L.G., Mosley-Thompson, E., Dansgaard, W., Grootes, P.M., 1986. The Little Ice Age as recorded in the stratigraphy of the tropical Quelccaya ice cap. Science 234, 361–364.

Thompson, L.G., Henderson, K.A., Mosley-Thompson, E., Lin, P.-N., 2000a. The tropical ice core record of ENSO. In: Diaz, H.F., Markgraf, V. (Eds.), El Niño and the Southern Oscillation: Multiscale Variability and Global and Regional Impacts. Cambridge University Press, Cambridge, pp. 325–356.

Thompson, L.G., Yao, T., Mosley-Thompson, E., Davis, M.E., Henderson, K.A., Lin, P.-N., 2000b. A high-resolution millennial record of the South Asian Monsoon from Himalayan ice cores. Science 289, 1916–1919.

Tudhope, A.W., Chilcott, C.P., McCulloch, M.T., Cook, E., Chappell, J., Ellam, Lea, R.M., Lough, D.W., Shimmield, J.M., 2001. Variability in the El Niño Southern Oscillation through a glacial-interglacial cycle. Science 291, 1511–1517.

Tziperman, E., Cane, M.A., Zebiak, E., Xue, Y., Blumenthal, B., 1998. Locking of El Niño's peak time to the end of the calendar year in the delayed oscillator picture of ENSO. Journal of Climate 11, 2191–2199.

Urban, F.E., Cole, J.E., Overpeck, J.T., 2000. Influence of mean climate change on climate variability from a 155-year tropical Pacific coral record. Nature 407, 989–993.

Walker, D., Owen, J.A.K., 1999. The characteristics and source of laminated mud at Lake Barrine, Northeast Australia. Quaternary Science Reviews 18, 1597–1624.

Walker, D., Head, M.J., Hancock, G.J., Murray, A.S., 2000. Establishing a chronology for the last 1000 years of laminated mud accumulation at Lake Barrine, a tropical upland Maar lake, northeastern Australia. The Holocene 10, 415–427.

Wang, L., Sarnthein, M., Erlenkeuser, H., Grimalt, J., Grootes, P., Heilig, S., Ivanova, E., Kienast, M., Pelejero, C., Plaumann, U., 1999. East Asian monsoon climate during the late Pleistocene: high-resolution sediment records from the South China Sea. Marine Geology 156, 245–284.

Webster, P.J., 1994. The role of hydrological processes in ocean–atmosphere interactions. Reviews of Geophysics 32, 427–476.

Woodroffe, C.D., Gagan, M.K., 2000. Coral microatolls from the central Pacific record late Holocene El Niño. Geophysical Research Letters 27, 1511–1514.

Woodroffe, C.D., Beech, M., Gagan, M.K., 2003. Mid-late Holocene El Niño variability in the equatorial Pacific from coral microatolls. Geophysical Research Letters 30, 1358, doi:10.1029/2002GL015868.

Yan, X.-H., Ho, C.-R., Zheng, Q., Klemas, V., 1992. Temperature and size variabilities of the Western Pacific Warm Pool. Science 258, 1643–1645.